Kardar-Parisi-Zhang universality in the phase distributions of one-dimensional exciton-polaritons

Davide Squizzato, Léonie Canet, and Anna Minguzzi
Univ. Grenoble Alpes, CNRS, LPMMC, 38000 Grenoble, France

(Received 11 December 2017; revised manuscript received 12 April 2018; published 31 May 2018)

Exciton-polaritons under driven-dissipative conditions exhibit a condensation transition that belongs to a different universality class from that of equilibrium Bose-Einstein condensates. By numerically solving the generalized Gross-Pitaevskii equation with realistic experimental parameters, we show that one-dimensional exciton-polaritons display fine features of Kardar-Parisi-Zhang (KPZ) dynamics. Beyond the scaling exponents, we show that their phase distribution follows the Tracy-Widom form predicted for KPZ growing interfaces. We moreover evidence a crossover to the stationary Baik-Rains statistics. We finally show that these features are unaffected on a certain timescale by the presence of a smooth disorder often present in experimental setups.

DOI: 10.1103/PhysRevB.97.195453

I. INTRODUCTION

Nonequilibrium systems exhibit a large variety of critical behaviors, some of which have no counterparts in equilibrium systems. This is the case for generic scale invariance, or self-organized criticality, which is realized, for instance, in the celebrated Kardar-Parisi-Zhang (KPZ) equation [1]. Originally derived to describe the kinetic roughening of growing interfaces, it arose in connection with an extremely large class of nonequilibrium or disordered systems [2,3] and has therefore become a paradigmatic model in physics for nonequilibrium scaling and phase transitions, and an archetype in mathematics of stochastic processes with non-Gaussian statistics [4].

Recently, KPZ dynamics has been unveiled in a condensed-matter system, namely the exciton-polariton condensate [5–10]. Exciton-polaritons (EPs) are elementary excitations arising in a semiconductor microcavity coupled to cavity photons. Since EPs have a finite lifetime, a stationary state is obtained under pumping. In these driven-dissipative conditions, the EP gas exhibits a nonequilibrium Bose-Einstein condensation transition, whose properties are investigated intensively [11]. It was shown that in a certain regime, the dynamics of the phase of the condensate can be mapped onto a KPZ equation. Whereas this finding was confirmed numerically in one dimension (1D) for well-chosen parameters [7], it was also suggested that this regime may not be accessible in current experimental systems.

In this paper, we reexamine the experimental realizability of KPZ universality in the 1D EP condensate. For this, we accurately model the system, taking into account realistic momentum-dependent losses and the quartic part of the dispersion of the polaritons. From this model, with actual experimental parameters, we demonstrate numerically that KPZ physics is observable under current experimental conditions. Moreover, beyond the KPZ scaling, we show that the exciton-polariton system displays other features that allow one unequivocally to infer its KPZ nature, in particular non-Gaussian distributions of the phase fluctuations.

Indeed, a breakthrough in the understanding of the statistical properties of a 1D KPZ interface was achieved in 2010 with the derivation of the exact distributions of the fluctuations of the height of the interface, followed by a wealth of other exact results [4]. These advances highlighted the remarkable features of the KPZ universality class: an unexpected connection with random matrix theory with the appearance of Tracy-Widom (TW) distributions [12], which are the distributions of the largest eigenvalues of matrices in the Gaussian orthogonal (GOE) or unitary ensemble (GUE). It was shown that the interface is sensitive to the global geometry, or equivalently to the initial conditions, defining three subclasses differing by their statistics: TW-GOE for flat [13,14], TW-GUE for sharp-wedge (i.e., δ-like) [15–17], or Baik-Rains (BR) distribution for stationary (i.e., Brownian) [18,19] initial conditions, while sharing the same KPZ scaling exponents.

This geometry-dependent universal behavior was first observed experimentally in turbulent liquid crystal [20,21]. However, despite recent progress, experimental observations of the KPZ universality are still scarce [22,23]. We show that the EP system stands as a promising candidate. We study numerically the fluctuations of the phase of the EP condensate, and we show that they precisely follow a TW-GOE distribution. Moreover, we show that a crossover from the TW-GOE to the BR distribution can be observed. This crossover is expected in a finite-size system when the correlation length becomes comparable with the system size but before finite-size effects begin to dominate, and it is in general difficult to access [24]. We show clear signatures of this crossover in the numerical distributions. Finally, we investigate the effect of disorder, which is unavoidable in experimental systems, and we show that KPZ physics is unaltered on a timescale related to the typical length scale of the disorder.

II. MODEL

A mean-field description of EPs under incoherent pumping was introduced in [25]. In this description, the dynamics of the polariton condensate wave function ϕ is given by [25]

$$i\,\partial_t\phi = \left[\mathcal{F}^{-1}[E_{\rm LP}(k)](x) + \frac{i}{2}(Rn_r - \gamma_l) + g|\phi^2|\right]\phi, \quad (1)$$

where the polaritonic reservoir density n_r is determined by the rate equation

$$\partial_t n_r = P - \gamma_r n_r - R n_r|\phi|^2. \quad (2)$$

$E_{\rm LP}(k)$ is the lower-polariton dispersion in momentum space, $\mathcal{F}^{-1}$ denoting the inverse Fourier transform, P is the pump, R is the amplification term, γ_l is the polariton loss rate, g is the polariton-polariton interaction strength, and γ_r is the reservoir loss rate. In the phenomenological model (1), the dispersion is usually approximated by a parabola of effective mass $m_{\rm LP}$ and a momentum-independent loss rate γ_l. In this work, in order to describe more accurately the experimental conditions, we include a momentum-dependent loss rate $\gamma(k) = \gamma_l + \gamma^{(2)}k^2$. The latter originates from localized excitons in the reservoir, and it is a now established experimental feature; see, e.g., [26]. Other types of momentum-dependent linewidths have also been reported, e.g., in the presence of a lattice [27]. The momentum-dependent loss rate yields an imaginary diffusion coefficient in the dynamics of the condensate, whose presence turns out to be crucial (see below). This excitonic effect is consistently taken into account in the dispersion relation by including quartic correction to the parabolic behavior [11]: $E_{\rm LP}(k) \simeq \frac{\hbar^2k^2}{2m_{\rm LP}} - \frac{1}{2\Omega}\big(\frac{\hbar^2k^2}{2m_{\rm LP}}\big)^2$.

In the case in which the timescales in the reservoir and in the condensate are well separated, one can solve the dynamics of the reservoir density to obtain an effective stochastic equation for the polaritonic condensate, taking into account the noise from both the condensate and the reservoir, which originates from the driven-dissipative nature of the fluid [7–9,28]. This effective equation reads in dimensionless form

$$\begin{aligned} i\partial_t\phi =& \big[-(1-iK_d)\nabla^2 - K_c^{(2)}\nabla^4 - (r_c - ir_d) \\ &+ (u_c - iu_d)|\phi|^2\big]\phi + \sqrt{\sigma}\xi, \end{aligned} \tag{3}$$

where we rescaled the time in units of $\hat{t} = \gamma_l^{-1}$, the space in units of $\hat{x} = (\hbar/2m_{\rm LP}\gamma_l)^{1/2}$, and the condensate wave function in units of $\hat{\phi} = [\gamma_r(p-1)/Rp]^{1/2}$, with $p = PR/(\gamma_l\gamma_r)$. The parameters in (3) are related to the parameters of the microscopic model via $r_d = u_d = (p-1)/2$, $u_c = \gamma_r g(p-1)/(R\gamma_l p)$, $\sigma = Rp(p+1)/[2\hat{x}\gamma_r(p-1)]$, and r_c is determined from the stationary-homogeneous solution of (3). The stochastic noise $\xi(x,t)$ is Gaussian with $\langle\xi(x,t)\xi^*(x',t')\rangle = 2\delta(x-x')\delta(t-t')$. Equation (3) is a generalized Gross-Pitaevskii equation (gGPE) with complex coefficients.

III. KPZ MAPPING

As shown in [10], by expressing the condensate wave function in a density-phase representation $\phi(x,t) = \sqrt{\rho(x,t)}\exp(i\theta(x,t))$ and performing a mean-field approximation over the density ρ at the level of the Keldysh action for the EP, one obtains that the dynamics of the phase field θ is ruled by the KPZ equation

$$\partial_t\theta = \nu\nabla^2\theta + \frac{\lambda}{2}(\nabla\theta)^2 + \sqrt{D}\eta\,, \tag{4}$$

where η is a white noise with $\langle\eta(x,t)\eta(x',t')\rangle = 2\delta(x-x')\delta(t-t')$, and $\nu = (K_c u_c/u_d + K_d)$, $\lambda = -2(K_c - K_d u_c/u_d)$, and $D = \sigma u_d(1+u_c^2/u_d^2)/2r_d$ [8]. The original KPZ equation describes the dynamics of the height of a stochastically growing interface. A 1D interface always roughens: it generically becomes scale-invariant. Its profile is usually characterized by the roughness, defined in term of θ as $w^2(L,t) = \langle\overline{\theta^2(x,t)} - \overline{\theta(x,t)}^2\rangle$, where $\overline{\cdot} = 1/L\int_x \cdot$ is the spatial average and $\langle\cdot\rangle$ the average over different realizations of the noise. The KPZ roughness is known to endow the Family-Vicsek scaling form [2,29]

$$w(L,t) \sim t^\beta F(Lt^{-1/z}) \sim \begin{cases} t^\beta, & t < T_s, \\ L^\chi, & t > T_s, \end{cases} \tag{5}$$

with $T_s \sim L^z$, and where the critical exponents take the exact values $\chi = 1/2$, $z = 3/2$, and $\beta = \chi/z = 1/3$ for the 1D KPZ universality class. The phase correlation function $\langle\theta(x,t)\theta(x',t')\rangle$ takes a similar scaling form and thus contains the same information about KPZ scaling.

IV. RESULTS

We numerically integrate the gGPE (3) using standard Monte Carlo sampling of the noise [30,31]. The parameters in this equation depend on the material. We use values typical for CdTe, used, e.g., in Grenoble experiments: $m_{\rm LP} = 4\times10^{-5}m_e$, $\gamma_l = 0.5\,{\rm ps}^{-1}$, $g = 7.59\times10^2\,{\rm ms}^{-1}$, $\gamma_r = 0.02\,{\rm ps}^{-1}$, $R = 400\,{\rm ms}^{-1}$, $p = 1.6$, $K_d = 0.45$, and $K_c^{(2)} = 2.5\times10^{-3}$. In each simulation, we determine the wave function $\phi(t,x)$ and extract its phase $\theta(t,x)$. We work in the low-noise regime, where the density fluctuations are negligible and topological defects are absent. In this regime, the phase can be uniquely unwound to obtain $\theta\in(-\infty,\infty)$.

A. KPZ scaling

To assess the presence of KPZ scaling in the system, we compute the roughness function $w^2(L,t)$ for the unwound phase θ of EPs and the first-order correlation function $\rho_1(x,t;x',t') = \langle\phi^*(x,t)\phi(x',t')\rangle$, determined directly from the condensate wave function. For the roughness, we obtain a perfect collapse onto the expected Family-Vicsek scaling form (5) using the KPZ exponents [32]. The equal-time and equal-space correlations show a stretched-exponential decay in good agreement with the KPZ theoretical properties, as first predicted in [7]. However, while in [7] KPZ scalings were observed only for appropriately chosen parameters, our calculations show that KPZ physics is present in current realistic experimental EP systems. They turn out to display a larger KPZ effective nonlinearity parameter $|g| \equiv |\lambda|(D/2\nu^3)^{1/2} \simeq 0.48$ than that used in [7], that facilitates the observation of the KPZ regime [32]. Let us stress that the inclusion of a momentum-dependent damping rate is crucial since it stabilizes the solution [33].

B. Beyond scaling: Tracy-Widom statistics

As emphasized in the introduction, unprecedented theoretical advances have yielded the exact probability distribution of the fluctuations of the 1D KPZ interface for sharp-wedge [15–17], flat [13,14], and stationary [18,19] initial conditions. It was shown that at long times, the interface height h behaves as $h(x,t) \simeq v_\infty t + (\Gamma t)^{1/3}\chi(x,t)$, with Γ and v_∞ nonuniversal parameters, and χ a random variable whose distribution is non-Gaussian, and exactly given by the TW-GUE, TW-GOE, and BR distribution, respectively [4].

To fully assess KPZ universality in EP systems, we use the gGPE simulations to obtain the probability distribution of a suitably rescaled, unwound phase $\tilde{\theta}(x,t) =$

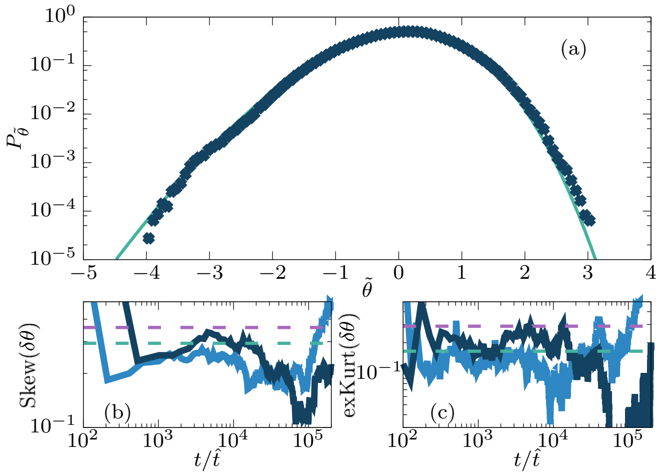

FIG. 1. (a) Distribution of $\tilde{\theta}$ for $L/\hat{x} = 2^{10}$, together with the theoretical centered GOE-TW distribution. (b) Skewness and (c) excess kurtosis (lower panel) of the phase field in the condensate for $L/\hat{x} = 2^9, 2^{10}$, together with the theoretical values for TW-GOE and BR statistics (green and purple dashed line, respectively). TW-GOE values are reached on a plateau around times $t/\hat{t} \simeq 10^4$.

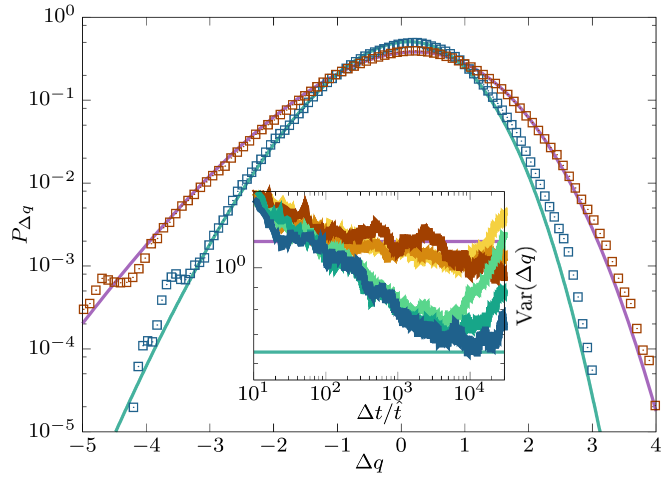

FIG. 2. Distribution of $\Delta q(x,t_0,\Delta t)$ for $\Delta t/t_0 = 10^3$ (light-green symbols) and $\Delta t/t_0 = 5 \times 10^{-3}$ (purple symbols) for $L/\hat{x} = 2^{10}$, together with the theoretical centered TW-GOE (green solid line) and BR (purple solid line) distributions [35]. Inset (same color code): numerical and theoretical values of var(Δq) for different initial times $t_0/\hat{t} = 10^2, 2 \times 10^4$ (blue and brown color-scale, respectively) and sizes $L/\hat{x} = 2^8, 2^9, 2^{10}$ (increasing from lighter to darker).

$\delta\theta(x,t)/(\Gamma t)^{1/3}$, where $\delta\theta(x,t) = [\theta(x,t) - \langle\overline{\theta}\rangle]$, thus subtracting the $v_\infty t$ term, and the parameter Γ is extracted from the numerical data according to the following procedure. First, we identify which probability distribution is realized in EP systems. This is assessed by computing universal ratios of cumulants of $\delta\theta(x,t)$, namely the skewness and the excess kurtosis, defined as $\text{Skew}(\delta\theta) = \langle\overline{\delta\theta^3}\rangle/\langle\overline{\delta\theta^2}\rangle^{3/2}$ and $\text{eKurt}(\delta\theta) = \langle\overline{\delta\theta^4}\rangle/\langle\overline{\delta\theta^2}\rangle^2 - 3$, respectively, where $\langle\overline{\delta\theta^n}\rangle = \langle\overline{(\theta - \langle\overline{\theta}\rangle)^n}\rangle$ [34]. These quantities are exactly zero for a Gaussian distribution and their universal ratios are known numerically at arbitrary precision for the distributions associated with the 1D KPZ equation [35,36]. Then, Γ is obtained from the relation $\Gamma = \lim_{t\to\infty} (\langle\overline{\delta\theta^2}\rangle/\text{var}_\chi)^{3/2}/t$, where var_χ is the theoretical value of the variance of the identified distribution [21,37].

In our data, we find that the cumulants reach stationary values on plateaus depending on the system size but roughly extending between $t = 10^3$ and 10^4 in units of $\hat{t}$. The values of these plateaus are compatible with TW-GOE distribution [see Fig. 1(b)]. We thus use the exact value of $\text{var}_{\text{TW-GOE}}$ to extract Γ, and we record the probability distribution of $\tilde{\theta}$ accumulated during the plateaus, which is represented in Fig. 1(a) [38]. We find that it is in excellent agreement with the TW-GOE distribution, thus providing convincing confirmation that KPZ dynamics is relevant in EP systems. We stress that, in the process of data treatment, the (space and time) phase unwinding is crucial in order to obtain unbounded fluctuations $\delta\theta$, which can acquire a $t^{1/3}$ scaling, as well as to eliminate unphysical 2π phase slips that may arise in the extraction of the phase from the condensate field. Furthermore, it is interesting to notice that the TW-GOE distribution is associated with a flat (i.e., spatially constant) initial condition for the KPZ height field, whereas in EP systems the initial phase of the condensate is essentially random, and not controllable, and moreover KPZ behavior sets in after a nonuniversal transient dynamics of the condensate.

C. Beyond scaling: Baik-Rains statistics

The TW distribution is associated with the growth regime of KPZ dynamics. In a finite-size system, a crossover to the stationary KPZ regime, characterized by the Baik-Rains distribution, is expected at sufficiently long times, but before finite-size effects dominate [21]. Indications of a change of regime are manifest in Fig. 1 since the skewness and excess Kurtosis depart from the plateaus at large times. However, this change is hindered by the noise and finite-size effects, which become more and more relevant as the correlation length becomes comparable to the system size.

To reduce finite-size effects and study this crossover, we follow Takeuchi [21] and introduce a new variable $\Delta q(x,t_0,\Delta t) = [\delta\theta(x,t_0 + \Delta t) - \delta\theta(x,t_0)]/(\Gamma t)^{1/3}$. Since this variable involves a phase difference, it does not require one to know the absolute phase, and is hence accessible in EP experiments. This variable is expected to display a TW-GOE distribution for $t_0 \to 0, \Delta t \to \infty$ and a BR distribution for $t_0 \to \infty, \Delta t \to 0$, with this precise ordering of the limits. The distribution of Δq is plotted in Fig. 2 for different ratios $\Delta t/t_0$. Both TW and BR distributions are clearly identified. Our analysis hence shows that the homogeneous EP condensate is an ideal playground to observe nontrivial out-of-equilibrium behavior associated with KPZ universality subclasses.

D. Influence of the system size

Most of the results are illustrated for systems of size $L/\hat{x} = 2^{10}$, i.e., about 1 mm. We have checked that KPZ features (both the scaling exponents and the phase distributions) are observable down to system sizes of the order of 50 microns

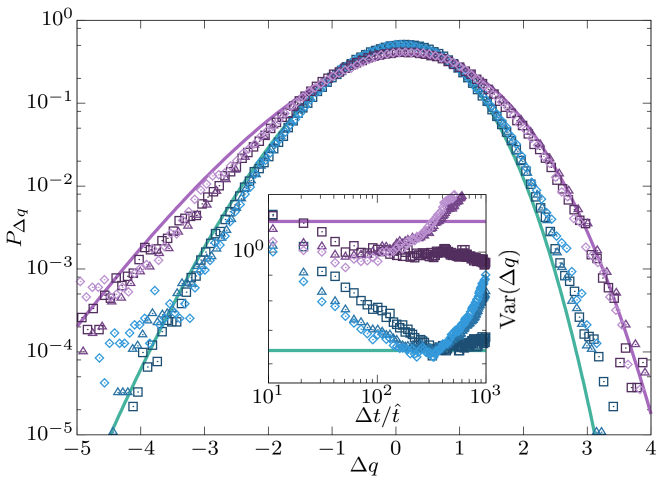

FIG. 3. Distribution of $\Delta q(x,t_0,\Delta t)$ for different disorder correlation lengths $\ell_d/L = 0.02, 0.07, 0.15$ (from lighter to darker) for $\Delta t/t_0 \simeq 10^2$ (blue symbols) and $\Delta t/t_0 \simeq 10^{-1}$ (purple symbols), with $L/\hat{x} = 2^{10}$. The solid lines correspond to centered TW-GOE (cyan) and BR (violet) theoretical distributions [35]. Inset (same parameters and color code): numerical and theoretical values for $\mathrm{var}(\Delta q)$.

[32]. This is remarkable since critical behaviors are generically expected in the limit of infinite system size.

E. Influence of the disorder

In experimental setups, the inhomogeneities due to cavity imperfections give rise to a static [39] disorder potential. We now investigate how this affects the KPZ physics. To model this disorder, we introduce a random-potential $V_d(x) = |\mathcal{F}^{-1}[V_d(p)](x)|$ with $\langle V_d(x)V_d(x')\rangle = G(x-x')$, $V_d(p) = V_0 e^{i\varphi} e^{-p^2\ell_d^2}$, and φ a uniformly distributed random variable in the range $[0,2\pi)$. By changing the correlation length ℓ_d, this describes any intermediate condition between a uniform potential for $\ell_d \to \infty$ and a white-noise disorder in the $\ell_d \to 0$ limit. We focus on finite values ℓ_d, corresponding to a smooth disorder typical of experiments. By means of the Keldysh formalism, one can show [40] that the inclusion of a static disorder in the Keldysh action leads to a nonlocal shift of the KPZ noise strength.

In the white-noise limit $\ell_d \to 0$ the presence of a disorder potential simply gives rise to a constant shift. However, in the case of a finite correlation length, the system is characterized by an additional microscopic length scale, which affects the phase fluctuations for times longer than the time scale $t_d \sim \ell_d^{2/3}$. We hence expect that for $t < t_d$, KPZ physics is still observable, while for $t > t_d$ the features of the disorder become dominant. The roughness and correlation functions computed in the presence of the disorder indeed confirm this picture [40]. We determined the distribution of the variable Δq in both regimes of large and small $\Delta t/t_0$. The results, presented in Fig. 3, show that for large $\Delta t/t_0$, the TW-GOE distribution is still accurately reproduced. Increasing t_0, the approach to the BR distribution is also clearly visible even if it cannot be fully attained, since t_0 is limited to t_d by the presence of the disorder.

V. CONCLUSIONS

We have shown that universal KPZ features can be observed under realistic experimental conditions in the dynamics of the phase of one-dimensional exciton polaritons. Our analysis shows that the full probability distributions of the phase fluctuations display universal KPZ properties, in particular its non-Gaussian nature, characterized by nonzero higher-order cumulants. We also observed a crossover between TW-GOE and BR distributions, allowing one to probe two well-known subclasses of 1D KPZ universality. Furthermore, we have shown that the presence of static disorder does not destroy KPZ physics on sufficiently small timescales. Even if the time-resolved measurement of the phase for the determination of the full distribution seems to be currently out of experimental reach, it would be enough to determine the first few cumulants to evidence KPZ distributions, exploiting for instance four-wave mixing processes, which have already been demonstrated in EPs [41]. In the context of ultracold atoms, higher-order cumulants of the phase have already been investigated experimentally [42,43]. The present analysis could stimulate new experimental protocols for the observation of KPZ properties in exciton-polaritons.

ACKNOWLEDGMENTS

The authors would like to thank Dario Ballarini, Denis Basko, Maxime Richard, and Alberto Rosso for inspiring discussions on both theoretical and experimental aspects. This work is supported by French state funds ANR-10-LABX-51-01 (Labex LANEF du Programme d'Investissements d'Avenir) and CNRS through the grant Infinity NEQ-DYN.

[1] M. Kardar, G. Parisi, and Y.-C. Zhang, Phys. Rev. Lett. **56**, 889 (1986).
[2] T. Halpin-Healy and Y.-C. Zhang, Phys. Rep. **254**, 215 (1995).
[3] J. Krug, Adv. Phys. **46**, 139 (1997).
[4] I. Corwin, Rand. Matrices: Theor. Appl. **01**, 1130001 (2012).
[5] K. Ji, V. N. Gladilin, and M. Wouters, Phys. Rev. B **91**, 045301 (2015).
[6] V. N. Gladilin, K. Ji, and M. Wouters, Phys. Rev. A **90**, 023615 (2014).
[7] L. He, L. M. Sieberer, E. Altman, and S. Diehl, Phys. Rev. B **92**, 155307 (2015).
[8] E. Altman, L. M. Sieberer, L. Chen, S. Diehl, and J. Toner, Phys. Rev. X **5**, 011017 (2015).
[9] M. Wouters and V. Savona, Phys. Rev. B **79**, 165302 (2009).
[10] L. M. Sieberer, M. Buchhold, and S. Diehl, Rep. Prog. Phys. **79**, 096001 (2016).
[11] I. Carusotto and C. Ciuti, Rev. Mod. Phys. **85**, 299 (2013).
[12] C. Tracy and H. Widom, Commun. Math. Phys. **159**, 151 (1994).

[13] P. Calabrese and P. Le Doussal, Phys. Rev. Lett. **106**, 250603 (2011).

[14] P. Le Doussal and P. Calabrese, J. Stat. Mech. (2012) P06001.

[15] G. Amir, I. Corwin, and J. Quastel, Commun. Pure Appl. Math. **64**, 466 (2011).

[16] T. Sasamoto and H. Spohn, Nucl. Phys. B **834**, 523 (2010).

[17] P. Calabrese, P. L. Doussal, and A. Rosso, Europhys. Lett. **90**, 20002 (2010).

[18] T. Imamura and T. Sasamoto, Phys. Rev. Lett. **108**, 190603 (2012).

[19] T. Imamura and T. Sasamoto, J. Stat. Phys. **150**, 908 (2013).

[20] K. A. Takeuchi and M. Sano, Phys. Rev. Lett. **104**, 230601 (2010).

[21] K. Takeuchi and M. Sano, J. Stat. Phys. **147**, 853 (2012).

[22] J. Ichi Wakita, H. Itoh, T. Matsuyama, and M. Matsushita, J. Phys. Soc. Jpn. **66**, 67 (1997).

[23] J. Maunuksela, M. Myllys, O.-P. Kähkönen, J. Timonen, N. Provatas, M. J. Alava, and T. Ala-Nissila, Phys. Rev. Lett. **79**, 1515 (1997).

[24] K. A. Takeuchi, Phys. Rev. Lett. **110**, 210604 (2013).

[25] M. Wouters and I. Carusotto, Phys. Rev. Lett. **99**, 140402 (2007).

[26] S. Klembt, P. Stepanov, T. Klein, A. Minguzzi, and M. Richard, Phys. Rev. Lett. **120**, 035301 (2018)

[27] F. Baboux, D. De Bernardis, V. Goblot, V. N. Gladilin, C. Gomez, E. Galopin, L. Le Gratiet, A. Lemaître, I. Sagnes, I. Carusotto, M. Wouters, A. Amo, and J. Bloch, arXiv:1707.05798.

[28] I. Carusotto and C. Ciuti, Phys. Rev. B **72**, 125335 (2005).

[29] F. Family and T. Vicsek, J. Phys. A **18**, L75 (1985).

[30] M. Werner and P. Drummond, J. Comput. Phys. **132**, 312 (1997).

[31] G. R. Dennis, J. J. Hope, and M. T. Johnsson, Comput. Phys. Commun. **184**, 201 (2013).

[32] See Supplemental Material at http://link.aps.org/supplemental/10.1103/PhysRevB.97.195453 for additional text and figures giving details on the scaling and on the effect of the system size.

[33] Note that a similar imaginary diffusion constant was introduced in [7] on an argument of relevance in the renormalization-group sense to stabilize the simulation.

[34] For the study of cumulants and phase distributions, the spatial average is not strictly needed, but it is used here to increase the statistics. One could work in a fixed point in space and just subtract the average of the phase over the noise realizations.

[35] M. Prähofer and H. Spohn, Phys. Rev. Lett. **84**, 4882 (2000).

[36] F. Bornemann, Math. Comput. **79**, 871 (2010).

[37] T. Halpin-Healy and Y. Lin, Phys. Rev. E **89**, 010103 (2014).

[38] Note that since $\lambda < 0$ for the EP system, the obtained distributions for $\tilde{\theta}$ are related to $P_{-\chi}$.

[39] A. Trichet, E. Durupt, F. Médard, S. Datta, A. Minguzzi, and M. Richard, Phys. Rev. B **88**, 121407 (2013).

[40] D. Squizzato, L. Canet, and A. Minguzzi (unpublished).

[41] V. Kohnle, Y. Leger, M. Wouters, M. Richard, M. T. Portella-Oberli, and B. Deveaud, Phys. Rev. B **86**, 064508 (2012).

[42] T. Schweigler, V. Kasper, S. Erne, I. Mazets, B. Rauer, F. Cataldini, T. Langen, T. Gasenzer, J. Berges, and J. Schmiedmayer, Nature (London) **545**, 323 (2017).

[43] T. Langen, S. Erne, R. Geiger, B. Rauer, T. Schweigler, M. Kuhnert, W. Rohringer, I. E. Mazets, T. Gasenzer, and J. Schmiedmayer, Science **348**, 207 (2015).